Magnesium Technology 2013
Edited by: Norbert Hort, Suveen N. Mathaudhu, Neale R. Neelameggham, and Martyn Alderman
TMS (The Minerals, Metals & Materials Society), 2013

Magnesium Technology 2013

Joining and Friction Processing

Magnesium Technology 2013
Edited by: Norbert Hort, Suveen N. Mathaudhu, Neale R. Neelameggham, and Martyn Alderman
TMS (The Minerals, Metals & Materials Society), 2013

Microstructure modification and performance improvement of Mg-RE alloys by friction stir processing

Yujuan Wu[1, 2], Liming Peng [1, 2*], Feiyan Zheng[1, 2], Xuewen Li[1, 2], Dejiang Li[1,2*], Wenjiang Ding [1, 2]
[1] *National Engineering Research Center of Light Alloy Net Forming, Shanghai Jiao Tong University, 800 Dongchuan Road, Shanghai 200240, PR China*
[2] *The State Key Laboratory of Metal Matrix Composites, Shanghai Jiao Tong University, 800 Dongchuan Road, Shanghai 200240, PR China*

Keywords: Friction stir processing, Mg–Gd–Zn–Zr, Mg-Gd-Ag-Zr, Mg-Nd-Zn-Zr, microstructure modification, performance improvement, LPSO structure

Abstract

Friction stir processing (FSP) is a severe plastic deformation (SPD) processing, which is very useful to refine grain size and secondary phase as well as change the texture of metal materials. Many FSP research were focused on aluminum alloys, while there are few reports on FSP of magnesium alloys, esp. on precipitation-hardening Mg-RE alloys. This paper overviewed the microstructures and mechanical properties of several FSPed Mg-RE alloys, such as Mg-Gd-Zn-Zr, Mg-Gd-Ag-Zr, and Mg-Nd-Zn-Zr with or without long period stacking ordering (LPSO) structure. The effects of processing parameters, such as rotation rate and traversing speed, on microstructure and mechanical properties were evaluated. It shows that FSP can effectively lend to performance improvement by microstructure modification, including obtaining remarkable finer and more homogenized grains, changing distribution and volume percentage of secondary phase etc.

Introduction

Magnesium (Mg) and its alloys, being the lightest structural metals, have remarkable potential applications in the aerospace, aircraft, and automotive industries for weight reduction in recent years [1]. However, the low strength, low ductility and poor creep resistance at increased temperatures restrict their wide applications. Recently, Mg alloys containing rare earth (RE) elements (especially heavy RE) have widely been developed and systematically investigated as promising materials with high strength and high creep resistance [2-4], which meet the demand for high temperature applications. Among them, Mg–RE–Zn/Cu/Al/Ni alloys (RE= Y, Dy, Ho, Er, Gd, Tb, Tm) alloys have attracted much attention, due to solution strengthening, aging strengthening [2-4] and long period stacking ordered (LPSO) structures strengthening and toughening [9-18].

At present, Mg–RE alloy parts are produced mainly by casting. However, coarser grains and eutectic at grain boundaries limit their mechanical properties and application, especially at higher temperatures. Therefore, it is need to modify the microstructures to enhance the mechanical properties, broadening its applications. Conventionally, heat treatment and various plastic deformation methods including severe plastic deformation (SPD) such as equal channel angular pressing (ECAP) [5] are applied to modify the microstructure of the Mg castings. However, the heat treatment for both the as-cast parts and pre-deformation parts at high temperature for lengthy time not only is time and cost consuming but also results in coarse grains as a result of their poor formability.

Friction stir processing (FSP), as one of SPD, is developed as a relatively novel metal working technique as based on the basic principle of friction stir welding (FSW) [19,20]. FSP causes SPD, material mixing and thermal exposure, so that it reduces intermetallic compounds size, grain size, and elimination of porosity through forging pressure, due to the combined influence of the tool tilt angle and shoulder diameter. At present, FSP has demonstrated as an effective process for producing the fine-grained heterogeneous bulk metal materials or surface composites, resulting from modifying the microstructure of metallic parent materials (PMs) and reinforced particles [19- 28].

In the past few years, several studies had been conducted to understand the effect of FSP on the microstructure and properties of Mg–Al–Zn (AZ) [21] and Mg–Al–Mn (AM) alloys [22,23]. It was reported that FSP resulted in remarkable grain refinement and significant breakup and dissolution of the coarse, network-like secondary eutectic phase–β-$Mg_{17}Al_{12}$, distributed at grain boundaries, which improved significantly the tensile properties of the casting, Recently, there is study on FSP for Mg-RE alloys, for example, WE43 [24], Mg-Gd-Y-Zr [27], Mg-Y-Zn [26], Mg-Nd-Zn-Zr [28] and Elektron 21 (ASTM EV31A) [29]. However, there are no reports on FSP for Mg-Gd-Ag-Zr [2,3] Mg-Gd-Zn-Zr [6-15] alloys.

Therefore, in this study, Mg-Gd-Zn-Zr, Mg-Gd-Ag-Zr, and Mg-Nd-Zn-Zr alloys ingots with or without LPSO structure were prepared by conventional ingot metallurgy (I/M). Then, FSP was used to these alloys for preparing fine-grained structure. The effects of FSP on the microstructure and mechanical properties of the alloy were investigated.

Experimental procedures

The alloys studied in the paper were GQ132K (Mg-13.1Gd-1.8Ag-0.48Zr, wt.%) , GZ132K (Mg-12.7Gd-1.9Zn- 0.52Zr, wt.%) and NZ20K (Mg-2.0Nd-0.3Zn-0.45Zr, wt.%). Alloys ingots were prepared by conventional ingot metallurgy (I/M). Pure Mg was

* Corresponding author at: Tel.: +86 21 54742911; fax: +86 21 34202794.
E-mail address:plm616@sjtu.edu.cn (Liming Peng); lidejiang@sjtu.edu.cn (Dejiang Li)

melted in an electric resistance furnace with a mild steel crucible under a protective gas (0.3% SF_6 and 99.7% CO_2). Pure Zn/Ag metal and Mg–25wt.%Gd / Mg-25 wt.% Nd were melted at about 973 K. Mg–30 wt. %Zr was added into the melt at about 1053 K. Finally, the melt was poured at about 1023 K into the mild steel mold preheated to 473 K. GZ132K and GQ132K alloys were cast into plates. NZ20K alloy were cast into cylinders. The alloy ingots were cooled in air, then cut into small specimens. The solid solution heat treatment for NZ20K and GQ132K alloys were carried out at 813K for 4h, and 723K for 12h, respectively, in a SX2-8-10-type high temperature heat treatment furnace, and immediately quenched in cold water. Then, the solution-treated ingot of NZ20K alloy was extruded to plate with extrusion ratio of 6 and temperature of 648 K.

The as-cast and as-extruded plates were machined to plates with thickness of 7 mm for FSP. A steel tool with a shoulder 22 mm in diameter, and a threaded cylindrical pin with 8 mm in diameter and 6 mm in length were used for the FSP experiment. A tool rotation rate of 800 rpm, and a traversing speed of 200 mm/min and the tool tilt angle of 2.8° were adopted. The aging treatment for as-FSPed GQ132K alloy was carried out in a furnace oil bath with constant temperature of 473K, and immediately quenched in cold water.

Tensile specimens with a gauge length of 10 mm, a width of 3 mm and a thickness of 1.5 mm were machined. For as-FSPed alloys, they were parallel to the FSP direction with the gauge being completely within the nugget zone. Four tensile specimens were measured in each zone. Tensile tests at room temperature were conducted on a Zwick T1-FR020TN A50 universal testing machine at a strain rate of 1.67×10^{-3} s^{-1}. Moreover, Vickers hardness tests were measured in the cross-sectional as-FSPed and aged samples by a HV-30 Vickers hardness tester with a 5 Kg load for 30 s.

Phase analysis was carried out by X-ray diffraction (Rogaku D/max 2550V) with angle from 10° to 90°, step size of 0.02° and step time of 15s and database is MDI Jade 5.0. To characterize the as-cast, as-extruded and as-FSPed microstructures for these three alloys, specimens etched by 4% HNO_3 and 96% ethanol were observed by optical microscopy (OM, Zeiss Axio Observer A1) and scanning electron microscopy (SEM, JEOL-7600F) at 10–20 KV equipped with an Oxford energy disperse X-ray spectrometer (EDS). For further study the microstructures and structures for the alloy, transmission electron microscopy (TEM, JEOL-2010) observations were carried out. The thin foils were thinned by a twin jet electropolishing in a solution of 5% $HClO_4$ and 95% ethanol under conditions of 20 mA, 75 V and 233 K and then by low energy beam ion thinning with the incidence angle of 4° and the voltage of 3.5 V for 0.5 h. Then, TEM observations were performed at 200 KV equipped with EDS.

Results and disscussion

Pre-FSPed microstructures

The microstructure of as-cast GQ132K alloy Fig. 1 shows OM and SEMmages of as-cast GQ132K alloy. The average grain size in the as-cast GQ132K alloy is about 55 μm. It shows that it consists of the α-Mg solid solution, the eutectic. Interestingly, there are two contrasts secondary phases in the eutectic, marked B and C in Fig. 1 (b).

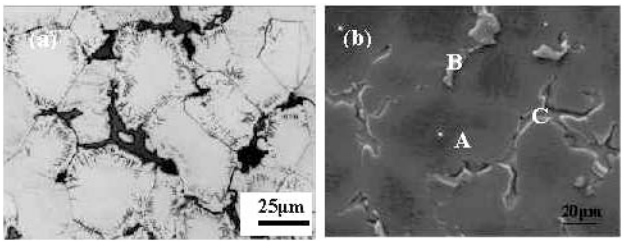

Fig. 1 (a) OM image, (b) SEM image of as-cast GZ132K alloy

By analysis of the EDS in the SEM mode, the compositions of Gd and Ag elements are different between the two phases. Among them, the B phase has higher Ag and lower Gd than C. However, both of them were established to Mg_5(Gd,Ag) phase, having a fcc structure with lattice constant of a = 2.22 nm, which will be reported in detail elsewhere.

In conclusion, the as-cast GZ132K alloy mainly consists of the α-Mg solid solution and β-Mg_5(Gd,Ag) phase. Interestingly, no LPSO structure is formed in the Mg-Gd-Ag-Zr alloy.

The microstructure of as-cast GZ132K alloy Fig. 2 shows OM, SEM, TEM images and corresponding selected-area electron diffraction (SAED) patterns of as-cast GZ132K alloy. The average grain size in the as-cast GZ132K alloy is about 60 μm. Fig. 2 (a) and (b) show that it consists of the α-Mg solid solution, the eutectic and lamellae [black structure within α-Mg matrix in Fig.2 (a)]. Fig.2 (c) and (d) show that the lamellae has a 14H-LPSO structure. There is coherent relationship, i.e., $(001)_{2H\text{-}Mg}$// $(0014)_{14H\text{-}LPSO}$ and $[001]_{2H\text{-}Mg}$// $[001]_{14H\text{-}LPSO}$. In addition, the lattice constants of the 2H-Mg and the 14H-type LPSO structure are estimated to be a = 0.325 nm, c = 0.520 nm, and a = 0.325 nm, c = 3.722 nm, respectively Furthermore, average chemical compositions of the 14H-type LPSO structure is Mg–8.10±1.0 at.% Zn–11.05±1.0 at.% Gd, by analysis of the EDS in the SEM mode [12]. Fig. 1(e)-(h) show that the secondary phase is the β-phase has a face-center cubic (fcc) structure with lattice constant of a = 0.719 nm [12].

In conclusion, the as-cast GZ132K alloy mainly consists of the α -Mg solid solution, the fine-lamellae with the 14H-type LPSO structure with matrix and the eutectic, in which the secondary phase is the β-phase [$(Mg,Zn)_3Gd$]. Therefore, the β-phase in the Mg-Gd-Zn-Zr alloy is different from that in Mg-Gd-Ag-Zr alloy in composition and lattice constant. There is almost same RE element and the third element contents (wt.%), compared to Mg-Gd-Ag-Zr alloy. However, no LPSO structure being formed in Mg-Gd-Ag-Zr alloy is possible to the causes of the different Zn an d Ag atom radius, solid solubility in Mg matrix, mixing enthalpy of the RE–X pair and the effect on stacking energy etc.

The microstructures of as-extruded NZ20K alloys Fig. 3 shows X-ray diffraction patterns of the as-extruded and as-FSPed NZ20K samples, respectively. It indicates that the microstructure of the as-extruded NZ20K alloy consists of α-Mg and precipitated phases $Mg_{12}Nd$.

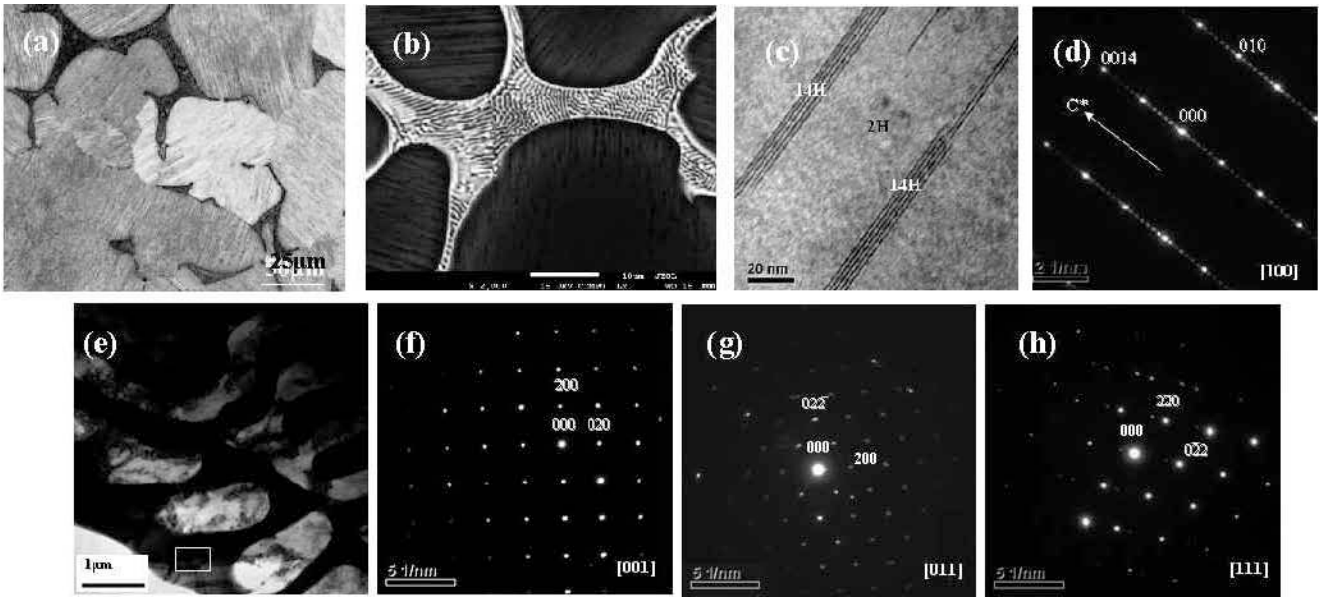

Fig. 2 (a) OM image, (b) SEM image, (c) Bright-field (BF) TEM image and (d) SAED patterns of the lamellar 14H-LPSO structure with electron beam // $[100]_{\alpha}$; (e) BF TEM image, (f)-(h) corresponding selected-area electron diffraction (SAED) patterns with the electron beams parallel to [001], [011] and [111] zones from TEM study for the secondary phase $[(Mg,Zn)_3Gd]$ in eutectic in as-cast GZ132K alloy, respectively

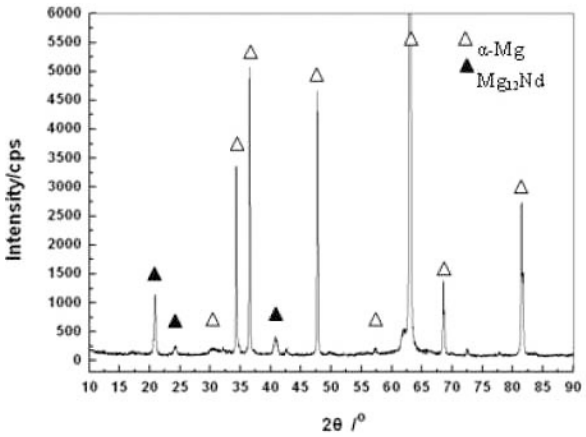

Fig. 3 X-ray diffraction pattern of as-extruded NZ20K alloy

Fig. 4 shows OM and SEM images of as-cast NZ20K alloy. The average grain size in the as-extruded alloy is about 21 μm. it indicates that the microstructure of the as-extruded NZ20K alloy consists of α-Mg and precipitated phases $Mg_{12}Nd$, combined with X-ray diffraction patterns analysis [30]. The $Mg_{12}Nd$ phase is formed by dynamic precipitation during hot-extrusion of the billet, as shown in Fig. 3(b), a large amount of grainy $Mg_{12}Nd$ distributes within the matrix, only a small amount of $Mg_{12}Nd$ distributes in the grain boundary.

Post-FSPed microstructures

The microstructure of as-FSPed GQ132K alloy Fig. 5 shows typical OM images of overall cross-section, TMAZ, and SZ for the as-FSPed GQ132K alloy. No defects in the joint, for example, tunnel, were detected in the sample, indicating the sound FSP parameter was achieved for the GQ132K alloy (rotation rate of 800 rpm, and a traversing speed of 200 mm/min). It shows distinct 4 regions: stir zone (SZ), thermo-mechanically affected zone (TMAZ), heat-affected zone (HAZ) and parent material (PM) after FSP in the alloy.

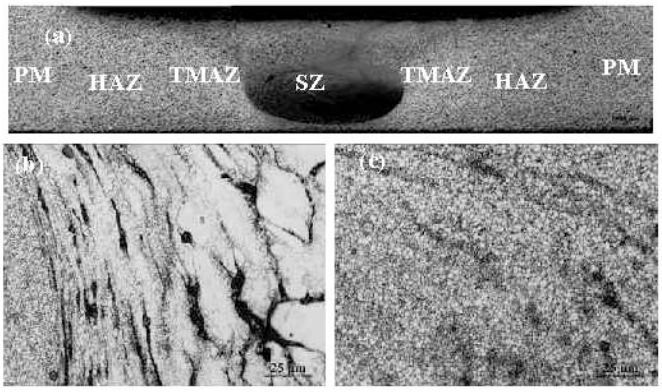

Fig. 5 Typical OM images of (a) overall cross-section, (b) TMAZ, and (c) SZ for the as-FSPed GQ132K alloy

After FSP, the primitive grains in SZ and TMAZ experience severe plastic deformation and dynamic recovery, while, the coarse grains have been broken. It is characterized by fine and equiaxed α-Mg grains in the SZ resulting from continuous dynamic recrystallization (CDRX) [Fig. 5(c)] , as compared with that in the PM [Fig. 1(a)].The grain size significantly decreases, and the average grain size is refined to about 1-4 μm from 55μm for the as-cast alloy [Fig. 5(c)]. While, it indicates that dynamic recrystallization (DRX) occurs in TMAZ during FSP; majority of

primitive grains experience SPD and are elongated and bent. Moreover, it indicates that the β-Mg_5(Gd,Ag) phase is severely elongated and bent in TMAZ, and it is broken and part of it is dissolved into matrix resulting in the volume percentage and size decreasing in SZ.

The microstructure of as-FSPed GZ132K alloy Fig. 6 shows OM and SEM images of the as-FSPed GZ132K alloy. It indicates that the as-cast alloy experiences severe plastic deformation in SZ and TMAZ. The β-phase [$(Mg,Zn)_3Gd$] and grains with lamellar 14H-LPSO structure are severely bent Correspondingly, the lamellar 14H-LPSO structure with α-Mg matrix occurs bend and kinking band appears, , as shown in Fig. 6(b) and (d). The grain sizes are refined and β- phase are brokenup and part of the particles are dissolved into matrix, compared to as- cast (PM) alloy. In SZ, the plastic deformation degree is increased, grain sizes are obviously refined from 60 μm to 1-3 μm, and the lamellar 14H-LPSO structure with matrix is much bent, as shown in Fig. 6(c) and (e), . Moreover, it shows that many lamellae with the 14H-type LPSO structure are formed within the fine-grains in SZ and TMAZ during FSP, like other plastic deformation processes such as extrusion [14], as shown in Fig. 6(b) - (e), which detailed content will be reported elsewhere.

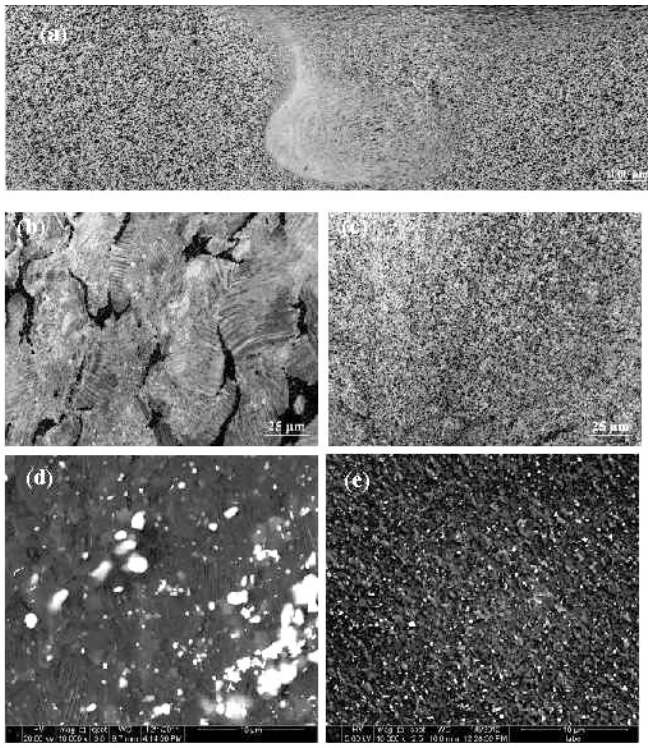

Fig. 6 Typical OM images of (a) overall cross-section, (b) TMAZ, and (c) SZ; SEM images of (d) thermo-mechanically affected zone (TMAZ) an (e) stir zone (SZ) for the as-FSPed GZ132K alloy

The microstructure of as-FSPed NZ20K alloy Fig. 7 shows typical OM images of the as-FSPed NZ20K alloy. It also shows distinct 4 regions like GQ132K alloy. It shows that the grain size significantly decreases in the SZ, as compared with that in the PM [Fig. 3(a)]. The average grain size in the as-extruded alloy is about 21 μm. After FSP, the microstructure of the SZ is characterized by fine and equiaxed α-Mg grains [Fig. 7(c)]. The average grain size in the SZ is measured to be 3-5μm. The primitive grains in SZ experience severe plastic deformation and dynamic recovery, while, the coarse grains have been broken. Therefore, it indicates that DRX occurs during FSP, but the time is too short for recrystallization grain to grow up, leading to significant grain refinement.

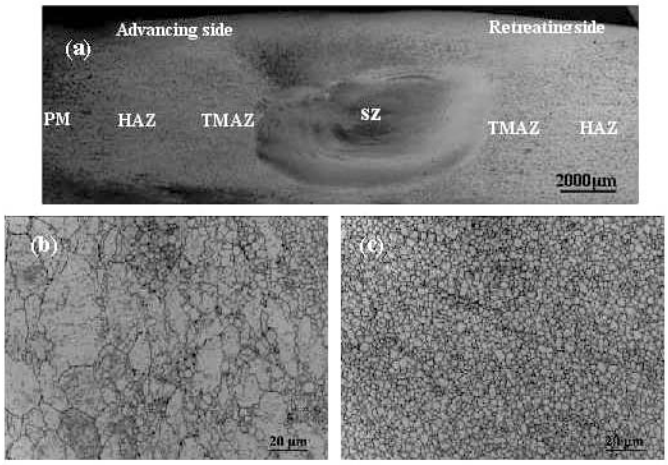

Fig. 7 Typical OM images of (a) overall cross-section, (b) TMAZ, and (c) SZ for the as-FSPed NZ20K alloy

TMAZ is found in the close vicinity of SZ, and also subjected to the thermal cycle and mechanical stress. DRX occurs in the part of zone and fine equiaxial grains nucleate and grew up, then, form the mixed zone of bulky grain and fine grain, as shown in Fig. 7 (b). The elongated and DRXed grain structures are characterized in the TMAZ and average grain size of TMAZ is 4.5-21μm.

Mechanical properties

Fig. 8 shows room-temperature tensile properties of the as-cast, solution-treated and as-FSPed GQ132K alloys. The as-cast alloy exhibits a yield tensile strength (YS) of 169 MPa, and ultimate tensile strength (UTS) of 241 MPa, and an elongation (δ) of 3.3%. After solution treatment at 773 K for 12 h, UTS and δ increase to 295 MPa, and 17.5 h, while, YS decreases little to 151MPa, mainly due to dissolution of coarse β-Mg_5(Gd,Ag) phase in grain boundaries which will be given elsewhere in the future. Interestingly, the tensile properties are obviously improved after FSP for the as-cast alloy without solution treatment, i.e., UTS, YS and δ increase to 344 MPa, 283 MPa and 20.2% from 241 MPa, 169 MPa and 3.3%. The reasons come from the dissolution, refinement and uniform distribution of β-Mg_5(Gd,Ag) phase, and grain refinement, otherwise, solution treatment would commonly increase the grain sizes for the as-cast alloy.

It can be concluded that FSP can effectively improve mechanical properties, by modify microstructure of Mg-RE alloys including refining grains and breaking and dissolution of particles.

Fig. 9 shows aging strengthening curves of PM and SZ for as-FSPed GQ132K alloy at 473K. The primary Vickers hardness of PM and SZ is 86.1 HV and 110.4 HV which increases 28% compared to PM. During aging, it is divided into 3 stages: under-aging, peak-aging and over-aging. They increase firstly, and arrive peak curves of 114.8 HV for 32 h, and 138.6 HV for 18h for

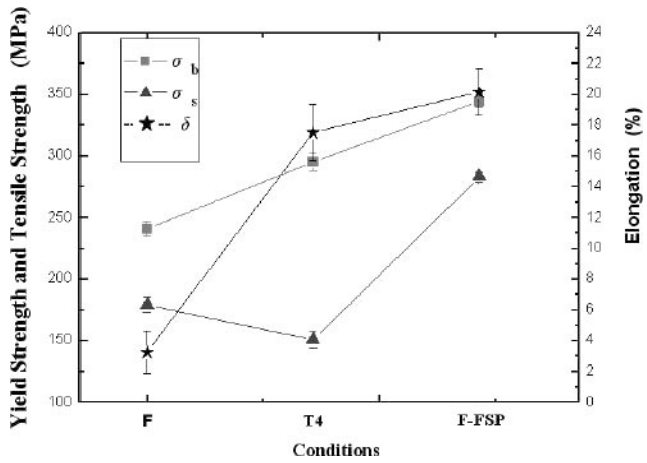

Fig. 8 Room-temperature tensile properties of the as-cast, solution-treated and as-FSPed GQ132K alloys

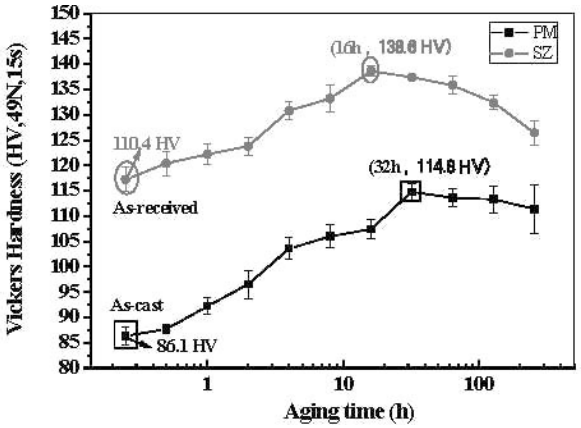

Fig. 9 Aging strengthening curves of PM and SZ for as-FSPed GQ132K alloy at 473K

PM and SZ, respectively. It indicates that the peak time for SZ shortens than PM and the peak hardness increases, which saving cost and time of aging and improving mechanical properties. The obvious aging strengthening for the aged GQ132K alloy is attributes to complex precipitation effect of ellipsoidal non-basal phase (β') and lamellar basal phase [3,4] in Mg-Gd-Ag(-Zr) sery alloy.

Conclusions

The conclusions are summarized as follows:

(1) It shows distinct 4 regions: stir zone (SZ), thermo-mechanically affected zone (TMAZ), heat-affected zone (HAZ) and parent material (PM) after FSP in the Mg-Gd-Zn-Zr, Mg-Gd-Ag-Zr, and Mg-Nd-Zn-Zr alloys.

(2) Continuous dynamic recrystallization (CDRX) occurs in SZ of, while, dynamic recrystallization (DRX) occurs in TMAZ during FSP for the Mg-RE alloys.

(3) To the as-cast GQ132K, as-cast GZ132K and as-extruded NZ20K alloys, the grain sizes are significantly refined from to 3-5μm, respectively, in SZ of FSP.

(4) The secondary eutectic phase in grain boundaries including β-Mg_5(Gd,Ag) phase in GQ132K, β-$(Mg,Zn)_3Gd$ phase in GZ132K alloys are severely deformed including being elongated and bent in TMAZ, and they are broken and part of them are dissolved into matrix resulting in the volume percentage and size decrease in SZ.

(5) In as-FSPed GZ132K alloy, the lamellar 14H-LPSO structure with primary α-Mg matrix occurs bend and kinking band appears in TMAZ. The lamellar 14H-LPSO structure with primary α-Mg matrix.

(6) It shows that many lamellae with the 14H-type LPSO structure are formed within the fine-grains in SZ and TMAZ during FSP.

(7) FSP can effectively improve mechanical properties, by modify microstructure of Mg-RE alloys including refining grains and breaking and dissolution of particles. For as-cast GQ132K, UTS, YS and δ increase to 344 MPa, 283 MPa and 20.2% from 241 MPa, 169 MPa and 3.3%. The Vickers hardness in SZ is improved from 86.1 HV in PM.

(8) The GQ132K exhibits obvious aging strengthening effect. For as-FSPed alloy, the peak time for SZ (16h) shortens than PM (32h) and the peak hardness increases from 114.8 HV to 138.6 HV.

Acknowledgements

The authors are grateful for the support f from National Natural Science Foundation of China (No.50971089), Shanghai Phospherus Program Project (No. 11QH1401200), China Postdoctoral Science Foundation (No.20090460615) and China Postdoctoral Science Special Foundation (201003267).

References

[1] A. Wendt, K. Weiss, A. Ben-Dov, et al., "Magnesium castings in aeronautics applications-Special requirements," *Magnesium Technology 2005*, (2005), 269-273.

[2] S.M. He, X.Q. Zeng, L.M. Peng et al., "Precipitation in a Mg–10Gd–3Y–0.4Zr(wt.%) alloy during isothermal aging at 250℃," *J. Alloy Comp.*, 421 (2006), 309-313.

[3] X. Gao, J.F. Nie, "Enhanced precipitation-hardening in Mg–Gd alloys containing Ag and Zn," *Scripta Mater.*, 58 (2008), 619-622.

[4] K. Yamada, H. Hoshikawa, S. Maki, "Enhanced age-hardening and formation of plate precipitates in Mg－Gd－Ag alloys," *Scripta Materialia*, 61 (2009): 636-639.

[5] B. Chen, D. L. Lin, X.Q. Zeng et al., "Microstructure and mechanical properties of ultrafine grained $Mg_{97}Y_2Zn_1$ alloy processed by Equal Channel Angular Pressing," *J. Alloy Comp.*, 440 (1-2) (2007), 94-100.

[6] Y. Kawamura, T. Morisaka, M. Yamasaki, "Structure and mechanical properties of rapidly solidified $Mg_{97}Zn_1RE_2$ Alloys," *Mater. Sci. Forum*, 419-422 (2003), 751-756.

[7] K. Amiya, T.Ohsuna, A. Inoue, "Long-period hexagonal structures in melt-spun $Mg_{97}Ln_2Y_1$ (Ln = Lanthanide metal) alloys," *Mater. Trans.*, 44 (10) (2003), 2151-2156.

[8] M. Yamasaki, T. Anan, S. Yoshimoto et al., "Mechanical properties of warm-extruded Mg–Zn–Gd alloy with coherent 14H long periodic stacking bordered structure precipitate," *Scripta Mater.*, 53 (2005), 799-803.

[9] Y. Kawamura, M. Yamasaki, "Formation and mechanical properties of $Mg_{97}Zn_1RE_2$ alloys with long-period stacking ordered structure," *Mater. Trans.*, 48 (11) (2007), 2986-2992.

[10] M. Yamasaki, M. Sasaki, M. Nishijima et al., "Formation of 14H long period stacking ordered structure and profuse stacking faults in Mg–Zn–Gd alloys during isothermal aging at high temperature," *Acta Mater.*, 55 (2007), 6798-6805.

[11] J.P.Li, Z. Yang, T. Liu et al., "Microstructures of extruded Mg–12Gd–1Zn–0.5Zr and Mg–12Gd–4Y–1Zn–0.5Zr alloys," *Scripta Mater.*, 56 (2007), 137-140.

[12] Y.J. Wu, D.L. Lin, X.Q. Zeng et al., "Formation of a lamellar 14H-type long period stacking ordered structure in an as-cast Mg-Gd-Zn-Zr alloy," *J. Mater. Sci.*, 44(2009):1607-1612.

[13] Y.J. Wu, X.Q. Zeng, D.L. Lin et al., " The microstructure evolution with lamellar 14H-type LPSO structure in an $Mg_{96.5}Gd_{2.5}Zn_1$ alloy during solid solution heat treatment at 773K," *J. Alloys Compd.*, 477 (2009):193-197.

[14] Y.J. Wu, L.M. Peng, D.L. Lin, et al., "A high-strength extruded Mg-Gd-Zn-Zr alloy with superplasticity," *J Mater. Res.*, 24(12)(2009): 3596-3602.

[15] W.J. Ding, Y.J. Wu, L.M. Peng, et al., " Formation of 14H-type long period stacking ordered structure in the as-cast and solid-solution-treated Mg-Gd-Zn-Zr alloys," *J Mater. Res.*, 24(5) (2009):1842-1854.

[16] H. Yokobayashi, K. Kishida, H. Inui, "Enrichment of Gd and Al atoms in the quadruple close packed planes and their in-plane long-range ordering in the long period stacking-ordered phase in the Mg-Al-Gd system, " *Acta Materialia* , 59(2011) : 7287-7299.

[17] P. P´erez , S. Gonz´alez, G. Garc´es, et al., "High-strength extruded $Mg_{96}Ni_2Y_1RE_1$ alloy exhibiting superplastic behaviour," *Mater. Sci. Eng. A,* 485 (2008), 194-199.

[18] Y. Kawamura, T. Kasahara, S. Izumi, et al., "Elevated temperature $Mg_{97}Y_2Cu_1$ alloy with long period ordered structure," *Scripta Mater.*, 2006, 55: 453-456

[19] R.S. Mishra, Z.Y. Ma, "Friction stir welding and processing, Materials Science and Engineering," *Materials Science and Engineering R,* 50(2005):1-78.

[20] R.S. Mishra, M.W. Mahoney, S.X. McFadden, et al., "High strain rate superplasticity in a friction stir processed 7075 Al alloy," *Scripta Mater.*, 42(2000):163-168.

[21] C.I. Chang, X.H. Du, J.C. Huang, "Achieving ultrafine grain size in Mg-Al-Zn alloy by friction stir processing," *Scripta Materialia*, 57(2007):209-212.

[22] R. Johnson, "Friction stir welding of magnesium alloys," *Mater. Sci. Forum*, 419-422(2003), 365-370.

[23] W.B. Lee, Y.M. Yeon, S.B. Jung, "Joint properties of friction stir welded AZ31B-H24 magnesium alloy, " Mater. Sci. Technol., 19(6)(2003), 785-790.

[24] M. Tsujikawa, S.W. Chung, M. Tanaka, et al., " High-strengthening of Mg - 5.5 mass % Y-4.3 mass % Zn cast alloy by friction stir processing," *Mater. Trans.*, 46 (12) (2005), 3081-3084.

[25] Q. YANG, B.L. XIAO, Z.Y. MA, "Influence of Process Parameters on Microstructure and Mechanical Properties of friction-Stir-Processed Mg-Gd-Y-Zr Casting," *Metallurgical and Materials transactions A*, 43A(2012), 2094-2109.

[26] S. W. Chung, M. Tsujikawa, T. Morishige, "Mechanical Properties on the Friction Stir Processed Cast Mg-1at.%Zn-2at.%Y Alloy," *Magnesium alloy 2007*,(2007), 299-305.

[27] B.L. Xiao, Q. Yang, J. Yang, "Enhanced mechanical properties of Mg-Gd-Y-Zr casting via friction stir processing," *Journal of Alloys and Compounds*, 509 (2011), 2879-2884.

[28] Z.L. Ning, F.Y. Cao, H.H Liu, et al., "Microstructure Analysis of Mg-2.54Nd-0.26Zn-0.32Zr Alloy, " R*are Metal Materials and Engineering*, 38(1)(2009):1997-2000.

[29] T. A. FREENEY, R.S. MISHRA, "Effect of Friction Stir Processing on Microstructure and Mechanical Properties of a Cast-Magnesium–Rare Earth Alloy," *Metallurgical and Materials transactions A*, 43A (2010), 73-84.

[30] F.Y. Zheng, Y.J. Wu, X.W. Li, "Microstructure and mechanical property evolution of Mg-2.0Nd-0.3Zn-1.0Zr alloy by friction stir processing," *Metallurgical and Materials transactions*, 2012, submitted.